NUMERICAL SIMULATION OF FLOW REVERSAL AT HIGH RAYLEIGH NUMBER IN A VERTICAL SQUARE DUCT – AN APPLICATION OF THE SPECTRAL METHOD

Kashif ALI[a], Shahzad AHMAD[*b], Muhammad ASHRAF[b], Muhammad Anwar KAMAL[c]

[a] *Department of Basic Sciences and Humanities, Muhammad Nawaz Sharif University of Engineering and Technology, Multan, Pakistan*

[b] *Centre for Advanced Studies in Pure and Applied Mathematics, Bahauddin Zakariya University, Multan, Pakistan*

[c] *Department of Mathematics, College of Science, King Saud University Riyadh, Saudia Arabia*

In this paper we numerically study the mixed convection in hydrodynamically as well as thermally developed incompressible laminar flow of nanofluids in a vertical square duct subject to the thermal boundary condition of constant heat flux per unit axial length with constant peripheral temperature at any cross section, using the spectral method and the finite difference method. We have considered three different water-based nanofluids containing Alumina, Titanium Oxide or Silver nanoparticles. We observe that the Rayleigh number remarkably reduces the fluid velocity and even the flow reversal may occur while developing an equi-temperature region for a small region in the centre of the duct. It has also been noted that, for Siler-water nanofluid, the nanoparticle volume fraction increases the Nusselt number more rapidly while slowly decreasing the fRe.

Key words: *Vertical duct; Water-based nanofluids; High Rayleigh number; Spectral method*

1. Introduction

Spectral methods are a class of techniques used in applied mathematics and scientific computing to numerically solve certain differential equations. In this method, the solution of the differential equation is written as a sum of certain basis functions (for example, as a Fourier series). The coefficients in the sum are then chosen in order to satisfy the differential equation as well as possible. Some of the basic ideas of the technique may be traced from Lanczos [1,2] and, Fox and Parker [3]. In the 1970s, the work of Orszag and others on the problems in fluid dynamics and meteorology played a very vital role to make the spectral methods very famous. Some other landmark works are Gottlieb and Orszag [4], Fornberg [5], Karniadakis and Sherwin [6] and, Calakli and Taubin [7].

The fluids that contain suspended nanoparticles such as metals or oxides are termed as nanofluids. It has been noted that no sedimentation occurs as the nano scale particles keep suspended in the base fluid. Similarly no significant increase in the pressure drop within the flow field takes place. The investigations reveal that the nanofluids exhibit enhanced thermal properties compared to the base fluid, and therefore have attracted the attention as a new generation of heat transfer fluids in plants, heat exchangers, building heating and in automotive cooling devices because of their excellent thermal performance (see Choi [8]). A lot of research is underway to apply nanofluids in environments where higher heat flux is encountered, and thus the conventional fluid is not capable of achieving the desired heat transfer. Several studies have been reported in the literature on the convective heat transfer in nanofluids; for example, Daungthongsuk and Wongwises [9], Trisaki and

E-mail address for correspondence: shahzadahmadbzu@gmail.com)
Wongwises[10] and, Wang and Mujumdar [11].

In the literature, many authors have analyzed the forced or mixed convection in rectangular ducts. Hartnett and Kostic [12] is an excellent review on the subject. Some authors have studied the combined forced and free convection in rectangular ducts by employing numerical or experimental methods. Cheng *et al* [13] have studied numerically the inlet region of a vertical rectangular duct with one wall kept at a higher temperature and the others at a lower temperature. The study has also been extended to the case of two or more walls kept at a higher temperature by Cheng *et al* [14]. Lee [15] has utilized the velocity–vorticity formulation to numerically solve the balance equations in the case of natural convection in a vertical rectangular duct with three adiabatic walls and the last one isothermal or subjected to a uniform heat flux. In Hwang et al. [16] employed the stream function method to solve numerically the governing equations for mixed convection in a horizontal square duct or in a horizontal circular tube. Alami and Campo [17] experimentally studied the flow and heat transfer in cooling flush-mounted ribbons in a channel, whereas the specific aspects of turbulent flows in rectangular ducts have been studied by Branislav et al. [18]. On the other hand, Ali et al. [19] numerically investigated the combined effect of thermal radiation and viscous dissipation in hydromagnetic micropolar fluid flow between two stretchable disks. MHD flow and heat transfer in the presence of a confined square cylinder was investigated by Farahi and Hossein [20], using the SM82 equations. Karthikeyan et al. [21] presented the **e**xperimental study of developing turbulent flow and heat transfer in ribbed convergent/divergent rectangular ducts. Fully developed laminar flow and heat transfer in a two-dimensional horizontal channel with staggered fins was numerically analyzed by Turgut and Arslan [22].

In this paper, we consider the mixed convection in hydrodynamically as well as thermally developed incompressible laminar flow of water-based nanofluid containing three different solid particles (Alumina, Titanium Oxide or Silver) in a vertical square duct subject to constant heat flux per unit axial length with constant peripheral temperature of the heated wall. We employ the spectral method as well as the finite difference method to solve the governing equations with appropriate boundary conditions, and compare the efficiency of two methods. The effect of the governing parameters on the velocity and temperature distributions is also discussed.

2. Mathematical formulation

We consider the hydrodynamically as well as thermally developed incompressible laminar flow of water-based nanofluid in a vertical square duct of side L, subject to constant heat flux per unit axial length with constant peripheral temperature at any cross section. The wall thickness of the duct is assumed to be negligible so that the assumption of infinite wall conductivity in the outward direction may be more realistic, which also means the same temperature on the outside duct surface and on the solid-fluid interface.

The velocity field for the problem is:

$\vec{V} = (0, 0, w(x, y))$,

and the governing equations of motion and heat transfer are:

Continuity Equation

$$\frac{\partial w}{\partial z} = 0, \tag{1}$$

Navier-Stokes Equations

$$\frac{\partial p}{\partial x}=\frac{\partial p}{\partial y}=0, \tag{2}$$

$$-\frac{\partial p}{\partial z}+\mu_{nf}\left(\frac{\partial^2 w}{\partial x^2}+\frac{\partial^2 w}{\partial y^2}\right)+g\left(T-T_w\right)\left(\rho\beta\right)_{nf}=0, \tag{3}$$

Heat Equation

$$w\frac{\partial T}{\partial z}=\alpha_{nf}\left(\frac{\partial^2 T}{\partial x^2}+\frac{\partial^2 T}{\partial y^2}+\frac{\partial^2 T}{\partial z^2}\right), \tag{4}$$

with boundary conditions

$$\left.\begin{aligned} w(x,0)=w(x,L)=w(0,y)=w(L,y)=0,\\ T(x,0)=T(x,L)=T(0,y)=T(L,y)=T_w(z),\end{aligned}\right\} \tag{5}$$

whereas,

$$\mu_{nf}=\frac{\mu_f}{(1-\varphi)^{2.5}},\ \rho_{nf}=(1-\varphi)\rho_f+\varphi\rho_s,\ \alpha_{nf}=\frac{k_{nf}}{\left(\rho c_p\right)_{nf}},$$

$$\left(\rho c_p\right)_{nf}=(1-\varphi)\left(\rho c_p\right)_f+\varphi\left(\rho c_p\right)_s,\ k_{nf}=\frac{\left(k_s+2k_f\right)-2\varphi\left(k_f-k_s\right)}{\left(k_s+2k_f\right)+\varphi\left(k_f-k_s\right)}k_f,$$

$$\left(\rho\beta\right)_{nf}=(1-\varphi)\left(\rho\beta\right)_f+\varphi\left(\rho\beta\right)_s,$$

with ϕ is the nanoparticle volume fraction parameter, ρ_s and ρ_f are, respectively, the densities of the solid fractions and of the fluid, c_p is the specific heat of the fluid at constant pressure, $\left(\rho c_p\right)_{nf}$ is the heat capacitance of the nanofluid, k_{nf} is the effective thermal conductivity of the nanofluid being approximated by the Maxwell-Garnett model, and finally β_s and β_f are the thermal expansion coefficients of the solid fractions and of the base fluid respectively.

Now eq. (2) implies $p=p(z)$, and for hydrodynamically developed flow,

$$\frac{dp}{dz}\equiv\text{Constant},$$

We consider the energy balance over a cross section of the duct and arrive at (Kays *et al* [23]):

$$\dot{Q}'dz=w_m\left(\rho c_p\right)_{nf}L^2dT_b \qquad \text{or} \qquad \frac{dT_b}{dz}=\frac{\dot{Q}'}{w_m\left(\rho c_p\right)_{nf}L^2}, \tag{6}$$

where $\dot{Q}'$ is the heat transfer rate per unit axial length, and T_b is the bulk temperature of the fluid defined as:

$$T_b=\frac{\int_0^L\int_0^L wT\,dx\,dy}{\int_0^L\int_0^L w\,dx\,dy}$$

We introduce the following dimensionless variables:

$$X=\frac{x}{L},Y=\frac{y}{L},W=-\frac{\mu_f w}{L^2\left(dp/dz\right)},\psi=\frac{k_f\left(T-T_w\right)}{\dot{Q}'}W_m \tag{7}$$

where

$$W_m = \int_0^1\int_0^1 W\,dXdY = -\frac{\mu_f w_m}{L^2\left(dp/dz\right)} \text{ with } w_m = \frac{1}{L^2}\int_0^L\int_0^L w\,dxdy = \int_0^1\int_0^1 w\,dXdY\,,$$

which implies

$$\frac{dp}{dz} = -\frac{\mu_f w_m}{L^2 W_m} \tag{8}$$

For thermally fully-developed flow subject to a constant heat transfer (per unit axial length) boundary condition, it is well known (Incropera and Dewitt [24]) that

$$\frac{\partial \psi}{\partial z} = 0 = \frac{\partial T}{\partial z} - \frac{dT_w}{dz} \text{ and } \frac{dT_w}{dz} = \frac{dT_b}{dz} \tag{9}$$

Combining eqs. (6) and (9)

$$\frac{\partial T}{\partial z} = \frac{dT_w}{dz} = \frac{dT_b}{dz} = \frac{\dot{Q}'}{w_m\left(\rho c_p\right)_{nf} L^2}, \text{ which implies } \frac{\partial^2 T}{\partial z^2} = 0$$

Therefore, the governing equations are reduced to:

$$1+\left(1-\phi\right)^{-2.5}\left(\frac{\partial^2 W}{\partial X^2}+\frac{\partial^2 W}{\partial Y^2}\right)+\left(1-\phi+\phi\frac{\left(\rho c_p\right)_s}{\left(\rho c_p\right)_f}\right)\left(1-\phi+\phi\frac{\left(\rho\beta\right)_s}{\left(\rho\beta\right)_f}\right)Ra\,\psi = 0 \tag{10}$$

$$\left(\frac{\partial^2 \psi}{\partial X^2}+\frac{\partial^2 \psi}{\partial Y^2}\right) = \frac{\left(k_s+2k_f\right)+\phi\left(k_f-k_s\right)}{\left(k_s+2k_f\right)-2\phi\left(k_f-k_s\right)}W, \tag{11}$$

where $Ra = \frac{\rho_f g\beta L^4}{\alpha_f \mu_f}\frac{dT_b}{dz}$ is the Rayleigh number (Dong and Ebadian [25]), with $\alpha_f = \frac{k_f}{\left(\rho c_p\right)_f}$ being the thermal diffusivity of the base-fluid. On the other hand, the boundary conditions are:

$$\left.\begin{aligned}\psi\left(X,0\right)=\psi\left(X,1\right)=\psi\left(0,Y\right)=\psi\left(1,Y\right)=0,\\ W\left(X,0\right)=W\left(X,1\right)=W\left(0,Y\right)=W\left(1,Y\right)=0.\end{aligned}\right\} \tag{12}$$

3. Numerical solution

We use both the spectral method and the finite difference method (FDM) to solve the coupled eqs. (10) and (11).

In the spectral method, we (considering the boundary conditions) set:

$$\left.\begin{aligned}W(X,Y) = \sum_{j=1}^{N}\sum_{k=1}^{N} a_{(j,k)}\sin\left(j\pi X\right)\sin\left(k\pi Y\right)\\ \psi(X,Y) = \sum_{j=1}^{N}\sum_{k=1}^{N} b_{(j,k)}\sin\left(j\pi X\right)\sin\left(k\pi Y\right)\end{aligned}\right\} \tag{13}$$

Now substituting eq. (13) in eqs. (10) and (11), and using

$$\int_0^1 \sin\left(m\pi t\right)\sin\left(n\pi t\right)dt = \begin{cases}0 & m\neq n\\ 1/2 & m=n,\end{cases} \qquad \text{(where } t \text{ is either } X \text{ or } Y\text{)}$$

the unknown coefficients are found to be:

$$\left.\begin{aligned} a_{j,k} &= \frac{1}{kj\pi^2}(1-\cos j\pi)(1-\cos k\pi)\Bigg/\left\{\frac{\Delta_1\Delta_2\Delta_3 Ra}{4\pi^2\left(j^2+k^2\right)} + 0.25(1-\phi)^{-2.5}\pi^2\left(j^2+k^2\right)\right\} \\ b_{j,k} &= -\frac{\Delta_3 a_{j,k}}{\pi^2\left(j^2+k^2\right)} \end{aligned}\right\} \quad (14)$$

where

$$\Delta_1 = 1-\phi+\phi\frac{\left(\rho c_p\right)_s}{\left(\rho c_p\right)_f}, \Delta_2 = 1-\phi+\phi\frac{(\rho\beta)_s}{(\rho\beta)_f}, \Delta_3 = \frac{\left(k_s+2k_f\right)+\phi\left(k_f-k_s\right)}{\left(k_s+2k_f\right)-2\phi\left(k_f-k_s\right)}$$

For the FDM, we first note that $\left(\frac{\partial^2}{\partial X^2}+\frac{\partial^2}{\partial Y^2}\right)F = G(X,Y)$ and (11) are the coupled Poisson equations, each being of the form:

where

$$F(X,Y) = W(X,Y) \quad \text{and}$$

$$G(X,Y) = -\left[1+\left(1-\phi+\phi\frac{\left(\rho c_p\right)_s}{\left(\rho c_p\right)_f}\right)\left(1-\phi+\phi\frac{(\rho\beta)_s}{(\rho\beta)_f}\right)Ra\,\psi(X,Y)\right](1-\phi)^{2.5}$$

for eq. (10), and $F(X,Y)=\psi(X,Y)$ and $G(X,Y)=\frac{\left(k_s+2k_f\right)+\phi\left(k_f-k_s\right)}{\left(k_s+2k_f\right)-2\phi\left(k_f-k_s\right)}W(X,Y)$

for eq. (11).

Both the coupled equations are discretized by using the compact nine-point scheme which is 4th order accurate, and is given by:

$$\left.\begin{aligned} &4\left(F_{i-1,j}+F_{i+1,j}+F_{i,j-1}+F_{i,j+1}\right)-20F_{i,j}+\left(F_{i-1,j-1}+F_{i-1,j+1}+F_{i+1,j-1}+F_{i+1,j+1}\right) \\ &=\frac{h^2}{2}\left(8G_{i,j}+G_{i-1,j}+G_{i+1,j}+G_{i,j-1}+G_{i,j+1}\right), \end{aligned}\right\} \quad (15)$$

where h is the uniform grid-size in both the $X, Y-$directions. The coupled linear algebraic systems corresponding to eq. (10) and (11), obtained by using eq. (15) are solved iteratively by employing the Successive over relaxation method (SOR).

Results and discussion

Physical quantities of our interest are the Darcy (or Moody) friction factor f and the Nusselt number Nu, given by:

$$f = -\frac{dp/dz\,L}{\rho_{nf}\,w_m^2/2} \text{ and } Nu = \frac{\dot{Q}'}{k_{nf}\left(T_w-T_b\right)}$$

Usually the friction factor is combined in a product with the Reynolds number ($\mathrm{Re}=\frac{\rho_f\,w_m}{\mu_f}L$) which, in view of eq. (7), can be written as:

$$f\,\mathrm{Re} = \left(\frac{\rho_f}{\rho_{nf}}\right)\frac{2}{W_m} \text{ and } N_u = \frac{W_m^2\left(k_f/k_{nf}\right)}{\int_0^1\int_0^1 W(X,Y)\psi(X,Y)\,dXdY}, \quad (16)$$

where $W_m = \int_0^1\int_0^1 W(X,Y)\,dXdY.$

We have considered three different water-based nanofluids containing Alumina, Titanium Oxide or Silver nanoparticles (Thermo-physical properties of water and the nanoparticles are given in the Tab. 1). For these nanofluids, we shall study the effects of the nanoparticle volume fraction parameter ϕ and the Rayleigh number *Ra* on the parameter *fRe* and the Nusselt number *Nu*, and also on the dimensionless temperature ψ and velocity fields W.

Tab. 2 gives the comparison of the Spectral method and the finite difference method (FDM) as well as the grid independence study for both the methods. It is clear that the numerical results for $f\,\mathrm{Re}$ and Nu converge as the number of grid points are increased. Moreover, compared with the FDM, more accurate results are obtained using the Spectral method at the coarser grids.

Figure 1 shows the effect of the relaxation parameter ω on the CPU time (in seconds) required to solve the eqs. (10) and (11) which are discretized by using the compact finite difference scheme given by eq. (15) and then solved by employing the SOR method. The nanoparticle volume fraction ϕ is fixed at 0.1 whereas four different values of the Rayleigh number Ra are considered ($Ra = 10000, 20000, 30000, 40000$) on the 51×51 grid. During the simulation process, we noted that the convergence was quite slow below $\omega = 1$ whereas the iterative process simply failed to converge at large Ra for $\omega > 1.5$. That is why, ω is chosen to lie in the range $(1 < \omega < 1.5)$ in the fig.1.

It is clear that the efficiency of the SOR method is remarkably influenced by the choice of omega, the lowest CPU time is above 4 seconds whereas the CPU time required to solve the problem with the above mentioned values of the parameters (ϕ *and Ra*) using the spectral method was noted to be just about 0.1 second, which depicts the supremacy of the Spectral method over the compact finite difference scheme.

Figures 2-3 give the dimensionless velocity and temperature distributions across the duct for $\phi = 0.05$ *and* $Ra = 10000$. It is obvious that the velocity in the centre of the duct is different both quantitatively and qualitatively. Due to the no slip condition, the velocity gradients are high near the walls. Moreover, the triangle like region near each corner of the duct is formed due to the influence of the two rigid boundaries. Figure 3, on the other hand, predicts an equi-temperature region in the middle of the duct at high Rayleigh number.

In order to observe the effect of the physical parameters on the velocity and temperature distribution, we consider the sections of the two surfaces (velocity and temperature) by the plane y = 0.5, thus, giving the temperature or velocity profiles in the middle of the duct. Figure 4 clearly shows that the increase in *Ra* remarkably reduces the fluid velocity to such an extent that the reverse flow may occur in the centre of the duct. Moreover, *Ra* decreases the temperature distribution while flattening the temperature profiles in the center of the duct, thus creating an equi-temperature region (fig. 5). On the other hand, nanoparticle volume fraction ϕ tends to eliminate the flow reversal in the duct while rendering the parabolic shape to the temperature profiles as shown in the figs. 6-7. In this way, the two physical parameters (ϕ and *Ra)* tend to neutralize the effect of each other.

Figures 8-9 show the influence of the nanoparticle volume fraction ϕ on $f\,\mathrm{Re}$ and Nu with $Ra = 10000$ for different nanoparticles (Alumina, Titanium Oxide and Silver).

It is clear from fig. 8 that, in general, ϕ decreases $f\,\mathrm{Re}$ for different nanoparticles but the sensitivity of $f\,\mathrm{Re}$ with ϕ is more pronounced for silver. On the other hand, there is no significant difference in the values of $f\,\mathrm{Re}$ corresponding to different ϕ, for the other two solid particles. Figure 9 predicts

that Nu is a linear function of ϕ for the three nanofluids, with Nu being least sensitive to ϕ in case of silver-water fluid.

Figures 10-11 demonstrate the effect of the Rayleigh number Ra on $f\,\mathrm{Re}$ and Nu with $\phi = 0.05$ for the nanofluids. It is clear that $f\,\mathrm{Re}$ for silver is always less than the corresponding values for the rest of the solid particles, for different Ra. On the other hand, there is not much difference in the values of Nu for different nanofluids as Ra increases.

Influence of the nanoparticle volume fraction ϕ on $f\,\mathrm{Re}$ and Nu with different Ra for silver is given in figs. 12-13 respectively. It is clear that $f\,\mathrm{Re}$ is more sensitive to ϕ at the smaller values of the later, and the sensitivity increases with Ra whereas Nu varies almost linearly with ϕ.

4. Conclusion

The purpose of this paper is to numerically study the mixed convection in the hydrodynamically as well as thermally developed flow in a vertical square duct, using the spectral method and the finite difference method (FDM). We have considered nanofluids with three different solid particles (Alumina, Titanium Oxide and Silver). Thermal boundary condition of constant heat flux per unit axial length with constant peripheral temperature of the heated wall is assumed. We notice the remarkable efficiency of the spectral method compared with the FDM, for solving the governing partial differential equations of the problem. We also observe that the Rayleigh number remarkably reduces the fluid velocity and, in the middle of the duct, flow reversal may even occur at high Rayleighnumber while flattening the temperature field (thus developing an equi-temperature region). It has been noted that the nanostructure of the fluid tends to discourage the effects of the mixed convection. Moreover, the Nusselt number Nu is found to be a linear function of the nanoparticle volume fraction parameter for the three nanofluids ϕ, with Nu being least sensitive to ϕ in case of silver-water fluid.

Acknowledgements

The authors are extremely grateful to the Higher Education Commission of Pakistan for the financial support to carry out this research.

Nomenclature

x, y, z	Cartesian coordinates, [m]
w	Velocity component, [ms^{-1}]
Ra	Rayleigh number, [-]
c_p	Specific heat, [m^2s^{-2}]
p	Pressure, [$kgm^{-1}s^{-2}$]
k_{nf}	Thermal conductivity of the nanofluid, [$kgms^{-3}K^{-1}$]
T	Temperature, [K]

Greek Symbols

μ_{nf}	Dynamic viscosity, [Nsm^{-2}]
ρ_{nf}	Density, $\left[kgm^{-3}\right]$
υ_{nf}	Kinematics viscosity, [m^2s^{-1}]
$(\rho c_p)_{nf}$	Heat capacitance of the nanofluid, [$kgm^{-1}s^{-2}K^{-1}$]
α_f	Thermal diffusivity , $\left[m^2s^{-1}\right]$

Table 1. Thermo-physical properties of water and nanoparticles

	Water	Copper(Cu)	Silver(Ag)	Alumina(Al_2O_3)	Titanium Oxide (TiO_2)
$\rho\left(kgm^{-3}\right)$	997.1	8933	10500	3970	4250
$C_p\left(Jkg^{-1}K^{-1}\right)$	4179	385	235	765	686.2
$k\left(Wm^{-1}K^{-1}\right)$	0.613	401	429	40	8.9538
$\beta\left(K^{-1}\right)$	21×10^{-5}	1.67×10^{-5}	1.89×10^{-5}	0.85×10^{-5}	0.9×10^{-5}

Table 2. Grid independency results (Siver-water, $\phi = 0.1, Ra = 10000$)

Grid	Spectral Method		Compact Finite Difference Scheme	
	Nu	f Re	Nu	f Re
31×31	37.1641	743.2869	36.7912	749.3896
41×41	37.1506	743.4911	36.9332	746.9790
61×61	37.1407	743.6182	37.0413	745.1820
81×81	37.1375	743.6551	37.0829	744.4852
101×101	37.1362	743.6697	37.0944	744.3808

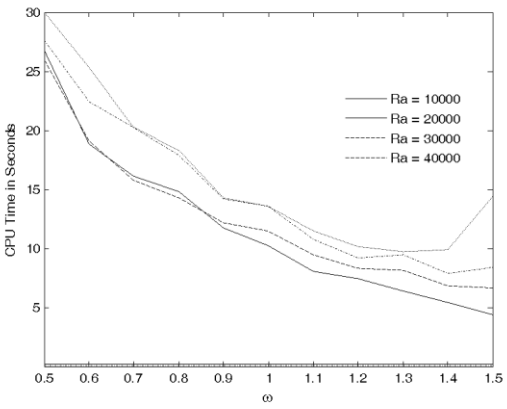

Figure 1. CPU Time for the SOR method against the relaxation parameter ω, for $\phi = 0.1$ and $Ra = 10000, 20000, 30000, 40000$.

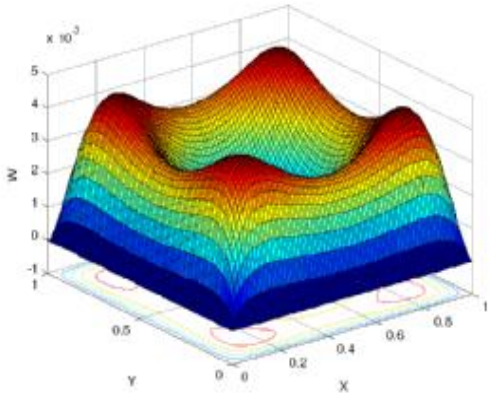

Figure 2. Dimensionless velocity W for silver for $\phi = 0.05$ and $Ra = 10000$.

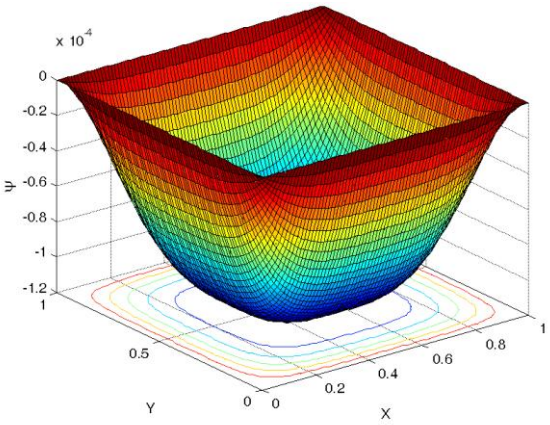

Figure 3. Dimensionless temperature ψ for silver for $\phi = 0.05$ *and* $Ra = 10000$.

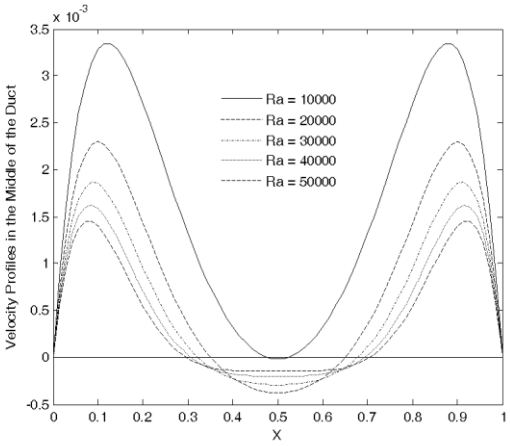

Figure 4. Velocity profiles in the middle of the duct for silver with $\phi = 0.05$ and various Ra.

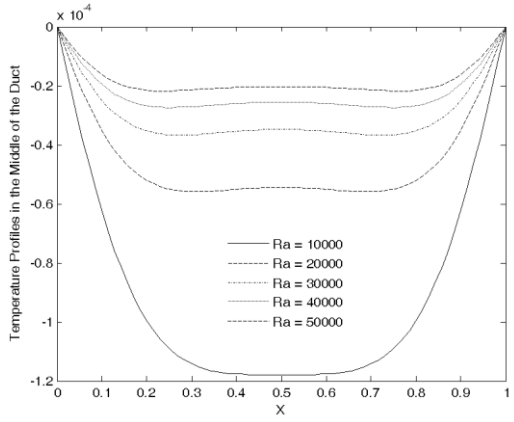

Figure 5. Temperature profiles in the middle of the duct for silver with $\phi = 0.05$ and various Ra.

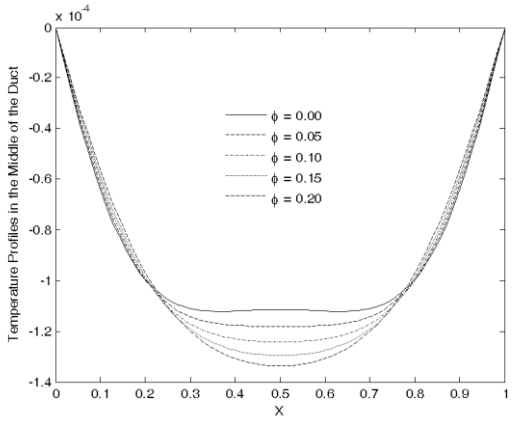

Figure 6. Temperature profiles in the middle of the duct for silver with $Ra = 10000$ and various ϕ.

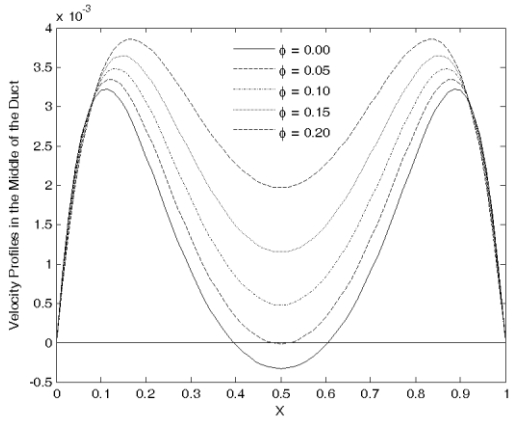

Figure 7. Velocity profiles in the middle of the duct for silver with $Ra = 10000$ and various ϕ.

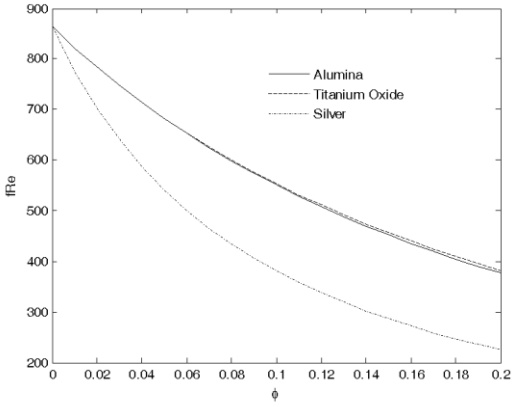

Figure 8. Influence of the nanoparticle volume fraction ϕ on $f\,\mathrm{Re}$ with $Ra = 10000$ for different nanoparticles.

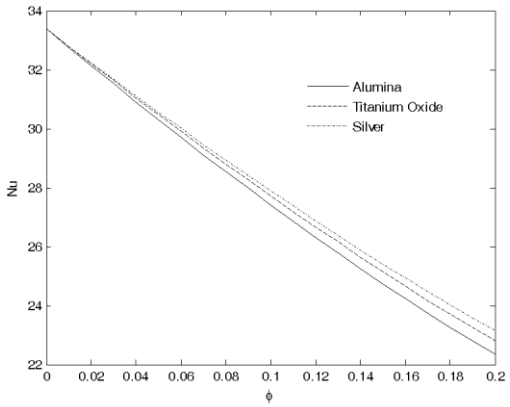

Figure 9. Influence of the nanoparticle volume fraction ϕ on Nu with $Ra = 10000$ for different nanoparticles.

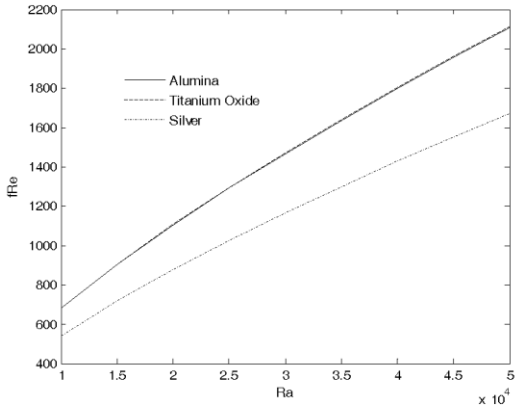

Figure 10. Influence of the Rayleigh number Ra on $f\,\mathrm{Re}$ with $\phi = 0.05$ for different nanoparticles.

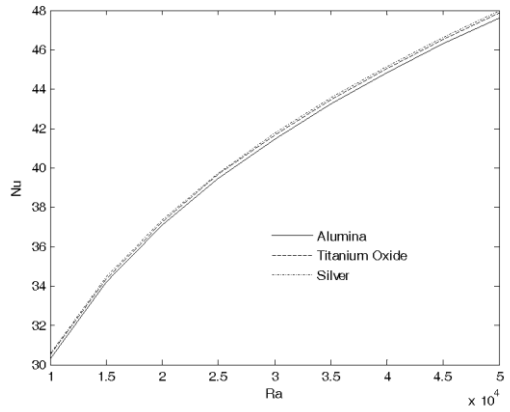

Figure 11. Influence of the Rayleigh number Ra on Nu with $\phi = 0.05$ for different nanoparticles.

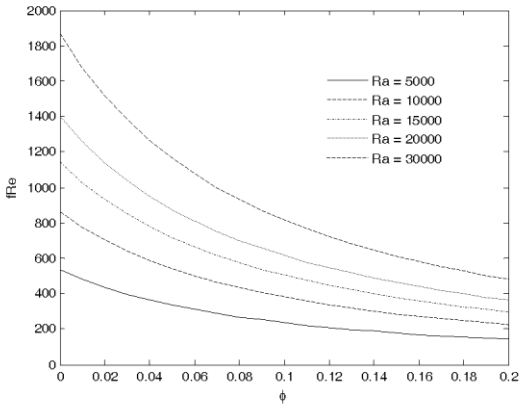

Figure 12. Influence of the nanoparticle volume fraction ϕ on $f\,\mathrm{Re}$ with different Ra for silver.

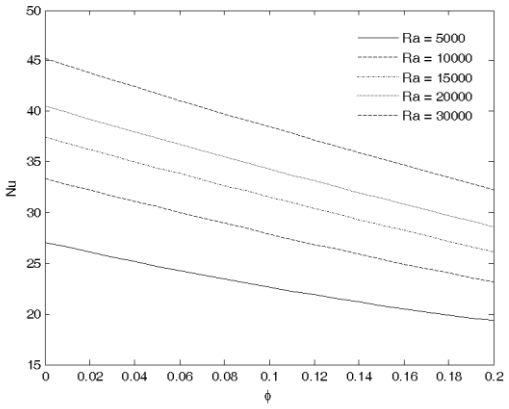

Figure 13. Influence of the nanoparticle volume fraction ϕ on Nu with different Ra for silver.

References

[1] Lanczos, C., Trigonometric interpolation of empirical and analytical functions, *J. Math. Phys.*, (1938), pp. 17

[2] Lanczos, C., *Applied Analysis*, Prentice-Hall, 1956

[3] Fox, L., *et al.*, *Chebyshev Polynomials in Numerical Analysis*, Oxford U. Press, 1968

[4] Gottlieb, D., Orszag, S. A., *Numerical Analysis of Spectral Methods: Theory and Applications*, *SIAM*, 1977

[5] Fornberg, B., *A Practical Guide to Pseudospectral Methods*, Cambridge University Press, 1996

[6] Karniadakis, G. E., Sherwin, S. J., *Spectral/hp Element Methods for CFD*, Oxford University Press, 1999

[7] Calakli, F., Taubin, G., *Smooth Signed Distance Surface Reconstruction*, Pacific Graphics, 2011

[8] Choi, S., Enhancing thermal conductivity of fluids with nanoparticles, *ASME Publications*, 66 (1995), pp. 99–105

[9] Daungthongsuk, W., Wongwises, S., A critical review of convective heat transfer nanofluids, *Renew Syst Energy Rev*, 11 (2007), pp. 797–817

[10] Trisaki, V., Wongwises, S., Critical review of heat transfer characteristics of nanofluids, *Renew Sust Energy Rev.*, 11 (2007), pp. 512–523

[11] Wang, X., Mujumdar, A. S., Heat transfer characteristics of nanofluids: A review, *Int J Therm Sci*. 46 (2007), pp. 1–19

[12] Hartnett, J. P., Kostic, M., Heat transfer to Newtonian and non-Newtonian fluids in rectangular ducts, *Adv. Heat Transfer*, 19 (1989), pp. 247–356

[13] Cheng, C. H., *et al.*, Buoyancy effect on the flow reversal of three-dimensional developing flow in a vertical rectangular duct—a parabolic model solution, *ASME J. Heat Transfer*, 117 (1995), pp. 236–241

[14] Cheng, C. H., *et al.*, Buoyancy-assisted flow reversal and convective heat transfer in entrance region of a vertical rectangular duct, *Int. J. Heat Fluid Flow*, 21 (2000), pp. 403–411

[15] Lee, K. T., Laminar natural convection heat and mass transfer in vertical rectangular ducts, *Int. J. Heat Mass Transfer*, 42 (1999), pp. 4523–4534

[16] Hwang, G. J., *et al.*, A computer-aided parametric analysis of mixed convection in ducts, *Int. J. Heat Mass Transfer*, 44 (2001), pp. 1857–1867

[17] Alami, N. A., Campo, A., Experimental investigation on flow and heat transfer for cooling flush-mounted ribbons in a channel: Application of an EHD active enhancement method, *Therm Sc*, 20(2016), No. 2, pp. 505-516

[18] Stanković, B.D., et al., Specific aspects of turbulent flow in rectangular ducts, *Therm Sci*, (2017), Suppl. 1, pp. xxx-xxx.

[19] Ali,.K., et al., On combined effect of thermal radiation and viscous dissipation in hydromagnetic micropolar fluid flow between two stretchable disks, Thermal Science, 2015 OnLine-First (00): pp. 96-96

[20] Farahi, S.M., Hossein, N.A., Investigation of MHD flow and heat transfer in the presence of a confined square cylinder using SM82 equations, THERMAL SCIENCE, Year 2017, Vol. 21, No. 2, pp. 889-899

[21] Karthikeyan, S., et al., Experimental study of developing turbulent flow and heat transfer in ribbed convergent/divergent rectangular ducts, Therm Sci, 19(2015), No. 6, pp. 2219-2231.

[22] Turgut, O., Arslan, K., Periodically fully developed laminar flow and heat transfer in a two-dimensional horizontal channel with staggered fins, Thermal Science, 2015 OnLine-First

(00):160-160.
[23] Kays, W. M., *et al.*, *Convective Heat and Mass Transfer (4th Edition)*, McGraw-Hill, New York, 2005
[24] Incropera, F. P., Dewitt, D. P., *Fundamentals of Heat and Mass Transfer*, John Wiley and Sons Ltd., 2011
[25] Dong, Z. F., Ebadian, M. A., Analysis of Combined Natural and Forced Convection in Vertical Semicircular Ducts with Radial Internal Fins, *Numerical Heat Transfer Applications*, 10 (1995), pp. 359-372